Chronic Alcohol Reduces Bone Formation Through Inhibiting Proliferation and Promoting Aging of Endothelial Cells in Type-H Vessels

Ao Chen
Nanjing Medical University
Xiaoting Li
Nanjing Medical University
Jingyu Zhao
Nanjing Medical University
Jiawen Zhou
Nanjing Medical University
Chunfeng Xie
Nanjing Medical University
Haiyun Chen
Nanjing Medical University
Qiuyi Wang
Nanjing Medical University
Rong Wang
Nanjing Medical University
Dengshun Miao
Nanjing Medical University
Jie Li
Xuzhou Medical University
Jianliang Jin (jinjianliang@njmu.edu.cn)
Nanjing Medical University https://orcid.org/0000-0003-3312-3210

Research

Keywords: BMP2, type-H vessel, endothelial cells, proliferation, Bmi-1, aging, p16, osteopenia

Posted Date: November 10th, 2021

DOI: https://doi.org/10.21203/rs.3.rs-1030987/v1

Chronic alcohol reduces bone formation through inhibiting proliferation and promoting aging of endothelial cells in type-H vessels

[1, *]Ao Chen, [3, *]Xiaoting Li, [1, *]Jingyu Zhao, [1, *]Jiawen Zhou, [3]Chunfeng Xie, [4]Haiyun Chen, [1]Qiuyi Wang, [1]Rong Wang,[1, 4]Dengshun Miao, [2, #]Jie Li and [1, #]Jianliang Jin

[1]Research Centre for Bone and Stem Cells, Department of Human Anatomy; Key Laboratory for Aging & Disease; The State Key Laboratory of Reproductive Medicine; Nanjing Medical University, Nanjing, Jiangsu, 211166; China

[2]Department of Orthopaedics, Xuzhou Central Hospital; The Xuzhou Clinical School of Xuzhou Medical University; The Xuzhou School of Clinical Medicine of Nanjing Medical University, Xuzhou, 221009; China

[3]Department of Nutrition and Food Safety, School of Public Health, Nanjing Medical University, Nanjing, Jiangsu, 211166; China

[4]The Research Center for Aging, Affiliated Friendship Plastic Surgery Hospital of Nanjing Medical University, Nanjing 210029; China

*These authors contributed equally to this work and should be considered co-first authors.

[#]Address all correspondence and requests for reprints to:

Dr. Jianliang Jin, M.D., Ph.D., Associated professor

E-mail: jinjianliang@njmu.edu.cn

Research Centre for Bone and Stem Cells

Department of Human Anatomy

Key Laboratory for Aging & Disease

The State Key Laboratory of Reproductive Medicine

Nanjing Medical University

No.101, Longmian Avenue, Jiangning District

Nanjing, Jiangsu 211166

China

Tel: 011-86-25-86869485

Dr. Jie Li, M.D., Ph.D.

E-mail: lijie87919@163.com

Department of Orthopaedics

Xuzhou Central Hospital

The Xuzhou Clinical School of Xuzhou Medical University

The Xuzhou School of Clinical Medicine of Nanjing Medical University

No. 199, Jiefang South Road

Xuzhou, Jiangsu 221009

China

Running title: Chronic alcohol inhibits type-H-vessel-dependent bone formation

Abstract

Background: Chronic alcohol is one of the leading risk factors for male osteoporosis. Angiogenesis and osteogenesis coupled by type-H vessels coordinate the biological process of bone homeostasis to prevent osteopenia. It is unknown whether alcohol inhibits type-H-vessel-dependent bone formation.

Aims: This study aimed to determine whether alcohol hampers proliferation and promotes aging of endothelial cells of type-H vessels, and whether alcohol inhibits the differentiation of bone marrow-mesenchymal stem cells (BM-MSCs) into osteoblasts through reducing the number and secretion of endothelial cells in type-H vessels.

Materials and Methods: Two-month-old mice fed with alcohol liquid diet (28% of calories) or normal liquid diet for two months. The tibias were isolated and detected with X-ray and micro-CT. Paraffin-embedded or frozen tibial sections were prepared and used for immunohistochemical or immunofluorescence staining respectively *in vivo*. Human Umbilical Vein Endothelial Cells (HUVECs) were treated with different-concentrated alcohol for 12 hours. The conditioned medium of the above HUVECs cells was collected to culture human BM-MSCs, which were induced to differentiate into osteoblasts *in vitro*.

Results: The alcoholic diet retarded the bone growth and lead to osteoporosis, impaired bone formation of osteoblasts, and decreased $CD31^{hi}EMCN^{hi}$ type-H-vessel formation through inhibiting proliferation and promoting aging of endothelial cells in mice. Alcohol treatment obviously increased the expression of p16, while significantly decreased the expression of Bmi-1, CDK6, Cyclin D, E2F1 and BMP2 compared to

vehicle. Alcohol inhibited the differentiation of BM-MSCs into osteoblasts through reducing the BMP2 secretion of endothelial cells in type-H vessels.

Conclusions: Alcoholic diet impaired $CD31^{hi}EMCN^{hi}$ type-H-vessel formation through inhibiting proliferation and promoting aging of endothelial cells via Bmi-1/p16 signaling, and inhibited the differentiation of BM-MSCs into osteoblasts through reducing the BMP2 secretion of endothelial cells in type-H vessels. It provides a basis for developing a new treatment strategy targeting aging endothelial cells of type-H-vessel to prevent alcoholic osteopenia.

Keywords: BMP2; type-H vessel; endothelial cells; proliferation; Bmi-1; aging; p16; osteopenia

1. Introduction

Osteoporosis is a metabolic disease characterized by decreased bone mineral density and the destruction of bone microstructure, which can lead to increased bone fragility and risk of fracture[1]. Chronic consumption of excessive alcohol eventually results in an osteopenic skeleton and increased risk for osteoporosis. Alcohol is one of the leading risk factors for male osteoporosis[2]. Compared with individuals without alcoholism, those with chronic alcohol abuse have significantly lower bone density (BMD) and lower bone volume in the femoral neck, showing thinner trabeculae, reduced range of bone-like surface and decreased average wall thickness of trabeculae[3, 4].

Blood vessels act as structural templates for bone development and also aggregate key elements of bone homeostasis into the osteogenic microenvironment, including minerals, growth factors and osteogenic progenitor cells[5]. Recent studies revealed that type-H vessels with strong positive expression of CD31 and endomucin (EMCN) proteins couple angiogenesis and osteogenesis[6]. Type-H vessels are surrounded by the transcription factors Runx2-positive and Osterix-positive osteoprogenitors, which determines that there is a close interaction between type-H vessels and osteogenic progenitor cells. Type-H vessels play an effective role in promoting bone regeneration. The osteogenic progenitor cells around type H vessels express Runx2 and Osterix at high levels to promote bone formation. Moreover, endothelial cells of type H vessels secrete many factors that trigger the proliferation and differentiation of osteoprogenitors to promote osteogenesis[7, 8]. Alcohol has been reported to have a

negative effect on angiogenesis[9, 10]. The anti-angiogenic effect of alcohol was found associated with excess reactive oxygen species (ROS) production[11]. However, whether alcohol hampers proliferation and promotes aging of endothelial cells of type-H vessels is still unclear, and whether alcohol inhibits the differentiation of bone marrow-mesenchymal stem cells (BM-MSCs) into osteoblasts through reducing the number and secretion of endothelial cells in type-H vessels remains unknown.

B lymphoma Mo-MLV insertion region 1 (Bmi-1) is a member of the polycomb family of transcriptional repressors [12, 13]. It could regulate cell cycle progression and prevent cell senescence through inhibiting $p16^{INK4a}$ (hereafter p16)*/Rb* and $p19^{AFR}$*/p53* pathways [14, 15]. Moreover, it also maintains mitochondrial function and redox homeostasis [13, 14]. In previous reports, inhibiting the expression of miR-125a could decrease the expression of p16, lead to the proliferation of vascular smooth muscle and endothelial cells, and then promote the remodeling of pulmonary artery[16]. However, whether Bmi-1 promotes proliferation and prevents aging of type-H vessels by inhibiting p16 and maintaining cell cycle progression is unclear.

In this study, we demonstrated the alcoholic diet impaired $CD31^{hi}EMCN^{hi}$ type-H-vessel formation through inhibiting proliferation and promoting aging of endothelial cells via Bmi-1/p16 signaling, and inhibited the differentiation of BM-MSCs into osteoblasts through reducing the BMP2 secretion of endothelial cells in type-H vessels. This study provides a basis for developing a new treatment strategy targeting aging

endothelial cells of type-H-vessel to prevent alcoholic osteopenia.

2. Materials and methods

2.1. Mice and experimental design

Eight-week-old C57BL/6J male mice were obtained from Vital River laboratories in Beijing of China and randomly assigned to two weight-matched groups (n=6/group) including an alcohol Lieber-DeCarli liquid diet (TROPHIC Animal Feed High-tech Co., Ltd., Nantong, Jiangsu, China) feeding group and a corresponding paired feeding group. By substituting carbohydrate calories with alcohol calories, alcohol was added to the Lieber-DeCarli liquid diet [17]. This alcohol liquid diet provides 28% of the calories and is equivalent to 5% alcohol by volume. The paired feeding group received the Lieber-DeCarli control liquid diet (TROPHIC) (TROPHIC Animal Feed High-tech Co., Ltd., China). Based on the previous day's dietary consumption, the paired feeding group was given equal calorie to its corresponding alcohol group. Alcohol and paired feeding diets were administered for two months. This study was carried out in strict accordance with the guidelines of the Institute for Laboratory Animal Research of Nanjing Medical University in Nanjing of China. The protocol was approved by the Committee on the Ethics of Animal Experiments of Nanjing Medical University (Permit Number: IACUC-1706001).

2.2. Radiography and micro–computed tomography

Four-month-old alcohol and pair-fed mice were euthanized to obtain the tibial tissue samples. Radiography was performed with a Faxitron machine (Model 805; Faxitron Bioptics, LLC, Tucson, AZ, USA) to observe tibias. A Lunar PIXImus densitometer (GE Lunar, Madison, WI, USA) was used to measure BMD of tibias. A SkyScan 1272 scanner and associated analysis software (Bruker, Kontich, Belgium) were used to conduct micro–computed tomography (micro-CT) of tibias as described[18] at Nanjing Medical University Medical Laboratory Animal Center.

2.3. Histology

Mouse tibias were fixed in 4% periodate-lysine-paraformaldehyde (PLP)[14, 15] for 24 hours and decalcified in a 10% ethylenediamine tetraacetic acid (EDTA) for 3-4 weeks. Samples were then embedded in paraffin, sectioned at 5 μm in thickness with a rotary microtome (Leica Microsystems Nussloch GmbH, Nubloch, Germany), and processed for histochemically staining of total collagen as previous described[15, 18] and Safranin O/fast green staining using a kit (#G1371, Beijing Solarbio science & technology Co., Ltd., Beijing, China), or for immunohistochemically staining [18, 19]. The samples were embedded in Optimal Cutting Temperature (O.C.T.) compound (#4583, SAKURA Finetek USA, Inc., CA, USA), and were sliced in thickness at 30 μm with a freezing microtome (Thermo Scientific Cryotome FSE Cryostats, Loughborough, Leicestershire) for immunofluorescence staining.

2.4. HBM-MSCs and HUVECs culture

Human Bone Mesenchymal Stem Cells (hBM-MSCs) were obtained from the American Type Culture Collection (PTA-1058; ATCC, VA, USA). The hBM-MSCs were cultured in medium including 85% (v/v) α-MEM, 15% (v/v) fetal bovine serum (FBS) (Gibco, Grand Island, NY, USA) and supplemented with 100 U/ml penicillin and 100 μg/ml streptomycin (Gibco, USA). Human Umbilical Vein Endothelial Cells (HUVECs) were obtained from the China Infrastructure of Cell Line Resources (Beijing, China) and cultured in endothelial cell medium (ECM) (#1001, ScienCell Research Laboratories, Inc., CA, USA) containing 10% FBS, Endothelial Cell Growth Supplement (ECGS) (#1052, ScienCell Research Laboratories, Inc., USA), 100 U ml^{-1} penicillin, and 100 μg ml^{-1} streptomycin as previously described[20]. Cells from the 3^{rd} passages to the 6^{th} passages were also used in the experiment, and the culture medium was changed every three days.

2.5. Immunofluorescence staining

Induced HUVECs were fixed with PLP solution[12] for 15 minutes and pre-incubated with serum. Primary antibodies against PECAM-1 (#557355, BD Pharmingen, NJ, USA), Endomucin (#DF13357, Affinity, Mel, AUS), Osterix (sc-393325, Santa Cruz Biotechnology Inc., Dallas, TX, USA), Runx2 (sc-390351, Santa Cruz Biotechnology Inc., USA), p16 (ab211542, Abcam, Cambridge, MA, USA), Bmp2 (18933-1-ap, Proteintech Group, Inc., IL, USA) and Bmi-1(66161-1-lg, Proteintech Group, Inc., USA) were used. After primary antibody incubation, bone sections and cells were

washed with phosphate buffered saline (PBS) (0.01 mM PO_4^{3-}, pH 7.4) for three times and incubated with appropriate Alexa Fluor-coupled secondary antibodies (Life Technologies Corporation, USA). Nuclei were labeled by DAPI (Sigma-Aldrich, St. Louis, MO, USA) and mounted with medium which prevents quenching of fluorescence (Vector Laboratories Inc., Burlingame, CA, USA).

2.6. Immunocytochemical staining

Bone sections were air-dried and endogenous peroxidase was blocked with 3% H_2O_2 and cells were pre-incubated with serum. Primary antibody against PCNA (sc-130920, Santa Cruz Biotechnology Inc., USA) and type-1 collagen (collagen 1) (ab88147, Abcam, USA) was used. After washing, bone sections were incubated with secondary antibody (biotinylated IgG; Sigma), washed, and processed using Vectastain ABC-HRP kits (Vector Laboratories Inc., USA).

2.7. *In vitro* assays of HUVECs proliferation and tube formation

We performed a Cell Counting Kit-8 (CCK-8) assay (#C0038, Beyotime Institute of Biotechnology, Shanghai, China) to assess cell proliferation as previously described[12]. For the CCK-8 assay, 2×10^3 HUVECs were inoculated into 96-well plates and incubated with alcohol for 12h. HUVECs viability was evaluated at 0h, 24h and 48h after alcohol treatment.

We assayed the tube formation with HUVECs on Matrigel (BD Bioscience, CA, USA).

2×10^4 HUVECs were incubated in a precooled 96-well plate and coated with 50 μL Matrigel. Cells were then treated with 0.5%, 3% or 5% alcohol for 12h, or with complete medium as the vehicle. After 12 h, endothelial cells linked by tubes were observed and quantified as previously described[21].

2.8. Osteogenic differentiation of hBM-MSCs *in vitro*

To identify osteogenic differentiation, the hBM-MSCs were cultured for 18 days in osteogenic medium of α-MEM from alcohol-treated HUVECs containing 15% (v/v) FBS, 100 U ml^{-1} penicillin, 100 μg ml^{-1} streptomycin, 2 mM L-glutamine, 10^{-8} M dexamethasone (Sigma-Aldrich, USA), 50 μg ml^{-1} ascorbic acid and 10 mM β-glycerophosphate (Sigma-Aldrich, USA) in a humidified 5% CO_2 incubator at 37°C [22, 23]. Medium was changed every three days. Induced hBM-MSCs were stained sequentially for alkaline phosphatase (ALP) by hydrolysis of naphtholphosphate, calcium nodules with alizarin red S[22, 23].

2.9. Cytology stainings

2.9.1. ALP staining

Induced hBM-MSCs were incubated in dark for 30 mins at room temperature in 100 mM Tris-maleate buffer containing naphthol AS-MX phosphate (0.2 mg ml^{-1}; Sigma-Aldrich, USA) dissolved in ethylene glycol monomethyl ether (Sigma-Aldrich, USA) as a substrate and Fast Red TR (0.4 mg ml^{-1}; Sigma-Aldrich, USA) as a stain for the reaction product [21, 24]. The hBM-MSCs were gently washed under running water

and left to dry.

2.9.2. Alizarin Red S staining for calcium nodules

Induced hBM-MSCs were exposed to a solution of Alizarin Red S (pH 6.2; 1 mg ml^{-1}) for 30 min at room temperature, after which hBM-MSCs were gently washed under running water and left to dry [21, 24].

2.10. Western blot

Western Blot analyses of Tibial bone marrow and HUVECs were performed following previously described methods [14, 25]. Primary antibodies against Bmp2 (18933-1-ap, Proteintech Group, Inc., USA), Osterix (sc-393325, Santa Cruz Biotechnology Inc., USA), Runx2 (sc-390351, Santa Cruz Biotechnology Inc., USA), ALP (11187-1-ap， Proteintech Group, Inc., USA), Bmi-1 (66161-1-lg, Proteintech Group, Inc., USA), CDK6 (#3136S, Cell Signaling Technology, Inc., Boston, MA, USA), Cyclin D (ab134175， Abcam, USA), E2F1 (ab179445, Abcam, USA) and β-actin (AP0714, Bioworld Technology, St. Louis Park, MN, USA) were used.

2.11. Statistical analysis

GraphPad Prism software (Version 9.0.0; GraphPad Software Inc., San Diego, CA, USA) was used to statistically analyze as previously described [12, 26]. Measurement data were described as mean ± SEM fold-change over control and analyzed by Student's *t*-test and one-way ANOVA to compare differences among groups.

Qualitative data were described as percentages and analyzed using chi-square tests as indicated [12, 14, 25]. P-values were two-sided and less than 0.05 was considered statistically significant.

3. Results

3.1. The alcoholic diet retards the bone growth and leads to osteoporosis in mice

To determine the effect of alcoholic diet on bone growth, the changes of bone growth and development in normal-diet and alcohol-diet mice were compared and analyzed by X-ray photography and Safranin O/fast green staining. Results showed that the tibial size, length (Fig. 1A-B) and growth plate thickness (Fig. 1C-D) of alcohol-diet mice were decreased when compared with those of normal-diet mice. In addition, PCNA positive chondrocytes were detected with immunohistochemistry and results showed that the proliferation of chondrocytes in alcohol-diet mice also decreased significantly in comparison with normal-diet mice (Fig. 1E-F). The changes of tibial bone volume and related indexes in mice fed with alcohol were observed by micro-CT (Fig. 1G) and total collagen staining (Fig. 1H). Compared with normal-diet mice, trabecular bone volume/bone tissue volume (BV/TV) percentage and bone mineral density (BMD) were downregulated, while trabecular separation (Tb.Sp) increased in alcohol-diet mice (Fig. 1I).

3.2. The alcoholic diet impairs bone formation of osteoblasts in mice

To investigate whether the inhibition of alcoholic diet on bone mass in mice was related to the change of osteogenesis ability, Runx2 immunofluorescence staining of tibial metaphyseal and immunohistochemical staining of type-1-collagen (collagen 1) were conducted. Results showed that the positive staining of Runx2 and collagen 1 in alcohol-diet mice were significantly downregulated when compared with normal diet mice (Fig. 2A-D). At the same time, the relative expression of osteogenesis-related proteins Bmp2, Osterix, Runx2 and ALP were detected by Western blots (Fig 2E-F) to observe the effect of alcoholic diet on bone formation in mice. Compared with normal-diet mice, the protein levels of Bmp2, Osterix, Runx2 and ALP were significantly decreased.

3.3. The alcoholic diet impairs $CD31^{hi}EMCN^{hi}$ type-H-vessel formation through inhibiting proliferation and promoting aging of endothelial cells

To determine whether disturbance of bone formation of osteoblasts after feeding with alcoholic diet was associated with decrease of type-H vessels, immunofluorescence staining of CD31 and EMCN were conducted to observe type-H vessels. Compared to normal-diet, alcohol-diet obviously decreased the number of $CD31^{hi}EMCN^{hi}$ type-H vessels. To further investigate whether the reduced number of type-H vessels caused by alcohol treatment attributed to the decreased proliferation and increased aging of endothelial cells in type-H vessels, the tube formation ability with Matrigel tube formation assay, cell proliferation with Cell Counting Kit-8 (CCK-8) assay, p16 expression with immunofluorescence staining, and proliferation-related proteins with

Western blots of HUVECs were detected. After HUVECs were treated with or without alcohol for 12 h, compared to vehicle, 3% or 5% alcohol treatment significantly decreased the total tube length; 5% alcohol treatment further decreased the total tube length in comparison with 3% alcohol treatment (Fig. 3C-D). After HUVECs were treated with or without alcohol for 12 h and then cultured for 48h, 3% or 5% alcohol treatment significantly inhibited cell proliferation compared to vehicle; 5% alcohol treatment further inhibited cell proliferation in comparison with 3% alcohol treatment (Fig. 3E). After HUVECs were treated with or without alcohol for 12 h, in comparison with vehicle, 0.5% alcohol treatment increased the expression of p16, while decreased the expression of Bmi-1, Cyclin D and E2F1; 3% or 5% alcohol treatment obviously increased the expression of p16, while significantly decreased the expression of Bmi-1, CDK6, Cyclin D and E2F1; 5% alcohol treatment further increased the expression of p16, while decreased the expression of Bmi-1, CDK6 and Cyclin D compared to 3% alcohol treatment (Fig. 3F-I).

3.4 Alcohol inhibits the differentiation of BM-MSCs into osteoblasts through reducing the BMP2 secretion of endothelial cells in type-H vessels

To investigate the effect of endothelial cells in type-H vessels on osteogenic differentiation of BM-MSCs, the conditioned medium of HUVECs cells treated with different concentrations of alcohol was collected to culture hBM-MSCs, which was then induced to differentiate into osteoblasts *in vitro*. Compared to vehicle, 3% or 5% alcohol treatment significantly decreased ALP and Alizarin red S positive calcium

nodules; 5% alcohol treatment further decreased ALP and Alizarin red S positive calcium nodules (Fig. 4A-D). *In vivo*, Alcohol-diet mice were characterized by a decreased number of Osterix-positive osteoprogenitors and/or osteoblasts (Fig. 3A-B). To determine whether alcohol reduced the BMP2 secretion of endothelial cells in type-H vessels, the BMP2 expression of aging endothelial cells was observed with immunofluorescence staining and detected with Western blot. Results showed that alcohol-diet mice had obviously decreased number of BMP2-positive or Bmi-1-positive endothelial cells and increased number of p16-positive endothelial cells in type-H vessels (Fig. 4E-H). After HUVECs were treated with or without alcohol for 12 h, in comparison with vehicle, 0.5%, 3% or 5% alcohol treatment obviously decreased the expression of Bmp2; 3% alcohol treatment further obviously decreased the expression of Bmp2 compared to 0.5% alcohol treatment; 5% alcohol treatment further decreased the expression of Bmp2 compared to 3% alcohol treatment (Fig. 4I-J). These results suggested that alcohol inhibited cell proliferation, promoted cell aging, and reduced the secretion of BMP2 of endothelial cells in type-H vessels, resulting in the decrease of osteogenic differentiation of BM-MSCs.

4. Discussion

This study demonstrated that the alcoholic diet retards the bone growth, impairs bone formation of osteoblasts and injures $CD31^{hi}EMCN^{hi}$ type-H-vessel formation through inhibiting proliferation and promoting aging of endothelial cells, leading to osteoporosis in mice. Meanwhile, alcohol inhibits the differentiation of BM-MSCs into osteoblasts through reducing the BMP2 secretion of endothelial cells in type-H vessels.

Chronic consumption of excessive alcohol eventually results in an osteopenic skeleton and an increase of risk for osteoporosis[2]. Alcohol-induced bone loss is characterized by damaged bone structure, decreased bone mass and increased fracture risk after alcohol abuse, which is mainly due to the direct and indirect effects of alcohol[27, 28]. Previous study has reported the positive effects of a small amount of alcohol on bones. In detail, light drinking (8g alcohol per day), mainly wine, was positively correlated with lumbar BMD and whole-body BMD of postmenopausal women[29]. In this study, low-concentrated alcohol had no effect on the proliferation of HUVECs. The conditioned medium of low-concentrated alcohol-treated HUVECs had no effect on the osteogenic differentiation of BM-MSCs *in vitro*. Although the effects of low-concentrated alcohol are controversial, chronic long-term drinking and binge drinking are harmful to bone tissue[30]. A large number of studies have confirmed that the animal model of long-term chronic drinking can be established by using Lieber-DeCarli liquid diet, which is reasonable to directly simulate human drinking[31]. It was previously reported that mice showed obvious osteoporotic phenotype under the same

feeding conditions as in this paper[17]. Based on the feed instructions of Lieber-DeCarli liquid alcohol diet, it provides 28% of the calories and is equivalent to 5% alcohol by volume. Consistent with our finding *in vivo* in this study, we found that when the alcohol concentration *in vitro* reached 5%, it significantly inhibited the proliferation and BMP2 secretion of endothelial cells and promoted their senescence.

In recent years, the coupling of angiogenesis and osteogenesis has become a new breakthrough in the treatment of osteoporosis[32]. Primary osteoporosis is characterized by a decrease in the number of sinuses and arterial capillaries in bone tissue, and the same phenomenon also occurs in postmenopausal osteoporosis[33]. Previous studies found that with aging-related bone loss in mice, the number of type-H vessels decreased, while the number of type-L vessels remained unchanged, and type-H vascular endothelial cells also decreased while the whole bone vascular endothelial cell content remained unchanged. And there is a coupling relationship with the content of osteoblasts in mice[6, 33]. The number of type-H vessels in the elderly is much less than that in the young, so the type-H vessels can be used as a sensitive indicator of bone aging and bone mass changes[7]. We found that high concentration of alcohol could promote the senescence of endothelial cells, and the aging endothelial cells would further affect the osteogenic differentiation of BM-MSCs, which may provide a new therapeutic target for aging osteoporosis. Previous studies found that through the inhibition of PI3K-Akt signaling pathway, high concentration of alcohol may alter many signaling pathways in HUVECs[34]. This suggests the effects of alcohol on cell

proliferation, differentiation, apoptosis and migration. The reduction of type-H vessels by alcohol plays an important role in alcohol-related bone loss[35]. We found that alcoholic diet inhibited proliferation and promoted aging of endothelial cells. Cyclin, cyclin-dependent kinases (CDKs) and cyclin-dependent kinase inhibitors (CKIs) play an important role in endothelial cell proliferation and migration[36]. P16 binds to cyclin/CDK complex and causes cell cycle arrest in G1 phase by inhibiting Rb phosphorylation mediated by CDK4/6. Meanwhile, dephosphorylated Rb binds to cell cycle-related transcription factor E2F and blocks its transcription activation domain[37]. In this study, alcohol regulates the proliferation and aging of HUVECs through this signal pathway. However, further study is needed to explore the crosstalk between vascularization and bone formation in ethanol-induced osteopenia.

Among all the BMPs, BMP2 has a strong osteogenic ability, which significantly increases the expression of osteocalcin. The short-term expression of BMP2 can irreversibly induce bone formation[38]. BMP2 is a key bone growth factor, which can stimulate osteoblast proliferation and induce BM-MSCs to differentiate into osteoblasts by inducing the expression of Runx2, Osterix and OCN genes. As specific transcription factors, Runx2 and OSX cooperatively regulate the expression of bone-specific genes, including ALP, type I collagen and OCN, which induce bone formation[1, 38, 39]. We found that BMP2 may be a key factor in coupling angiogenesis and osteogenesis. In addition, when bone is injured, the fracture area is surrounded by hematoma. Local hypoxia induces upregulation of BMP2 in endothelial cells to promote osteogenesis.

Hypoxia inducible factor-1α (HIF-1α) accumulates in osteoblasts, activating HIF-1α signal pathway to specifically activate endothelial cells, which leads to VEGF-A production, further promotes type-H-vessel formation and secretion of BMP2, and accelerates bone formation[6, 40]. BMPs play an important role in bone formation and fracture healing[41]. Recently, it has been reported that the local and temporary applications of BMP2 stimulate the activation of skeletal stem cells, combined with low level of a CSF1 antagonist inhibits bone resorption, and restores bone regeneration in aged mice[42]. BMP2 is used as an auxiliary drug for fracture healing in clinic[43]. Commercially available BMPs provide a substitute for autologous bone graft for the treatment of tibial nonunion. The recombinant human BMP2 has been widely studied in various preclinical and clinical studies, but the clinical research on nonunion is limited[44]. In addition, some studies have confirmed that alcohol could affect the expression of BMP2[45]. Our results demonstrated that alcohol inhibited the differentiation of BM-MSCs into osteoblasts through reducing the BMP2 secretion of endothelial cells in type-H vessels. However, whether BMP2 expression is regulated by Bmi-1/p16 signalling pathway in aging endothelial cells of type-H vessels needs further study.

5. Conclusions

In conclusion, the alcoholic diet impaired type-H-vessel formation through inhibiting proliferation and promoting aging of endothelial cells via Bmi-1/p16 signaling, and curbed the osteogenic differentiation of BM-MSCs through reducing the BMP2

secretion of endothelial cells in type-H vessels. It provides a basis for developing a new treatment strategy targeting aging endothelial cells of type-H-vessel to prevent alcoholic osteopenia.

Abbreviations

α-MEM: Minimum Essential Medium α

ALP: Alkaline phosphatase

BMD: Bone density

Bmi-1: B lymphoma Mo-MLV insertion region 1

BM-MSCs: Bone marrow-mesenchymal stem cells

BMP2: Bone morphogenetic protein-2

BV/TV: Trabecular bone volume/bone tissue volume

CCK-8: Cell counting kit-8

CD31/ PECAM-1: Platelet endothelial cell adhesion molecule-1

CDK6: Cyclin-dependent kinase 6

CKIs: Cyclin-dependent kinase inhibitors

CO_2: Carbon dioxide

CSF1: Colony stimulating factor 1

CT: Computed tomography

DAPI: 4',6-diamidino-2-phenylindole

E2F1: E2F transcription factor 1

ECGS: Endothelial cell growth supplement

ECM: Endothelial cell medium

EDTA: Ethylenediamine tetraacetic acid

EMCN: Endomucin

FBS: Fetal bovine serum

H_2O_2: Hydrogen peroxide

hBM-MSCs: Human bone mesenchymal stem cells

HIF-1α: Hypoxia inducible factor-1α

HUVECs: Human umbilical vein endothelial cells

OCN: Osteocalcin

O.C.T.: Optimal cutting temperature

OSX: Osterix

P16: $P16^{Ink4a}$

PBS: Phosphate buffered saline

PCNA: Proliferating cell nuclear antigen

PI3K: Phosphatidylinositol 3 kinase

PLP: Periodate-lysine-paraformaldehyde

ROS: Reactive oxygen species

Runx2: Runt-related transcription factor 2

Tb.N: Trabecular number

Tb.Sp: Trabecular separation

Tb.Th: Trabecular thickness

VEGF: Vascular endothelial growth factor

Acknowledgements

This work was supported by grants from the National Natural Science Foundation of China (81871097 and 81571371 to J.J., 81602839 to X.L. and 81730066 to D.M.), the

"Qinglan project" funded by Jiangsu Universities (2020-10 to J.J.), the Natural Science Foundation of Jiangsu Province (BK20151554 to J.J.), the Scientific Research Project of Jiangsu Health Commission (H2019023 to J.L.), and the Xuzhou Science and Technology Project (KC19152 to J.L.).

Author Contribution statement

Conceptualization, J.J., J.L. and D.M.; Methodology, A.C., X.L., J.Z., J.Z., C.X., H.C., Q.W., R.W., D.M., J.L. and J.J.; Software, A.C., X.L., J.Z., J.Z., C.X., J.L. and J.J.; Validation, A.C., X.L., J.Z., H.C., Q.W., R.W., J.L. and J.J.; Data Analysis, A.C., X.L., J.Z., H.C., J.L. and J.J.; Writing – Original Draft, A.C., J.J. and X.L., with help from the other authors; Writing – Review & Editing, J.J., J.L. and D.M., with help from the other authors; Project Administration and Supervision, J.J., X.L., J.L. and D.M.; Funding Acquisition, J.J., J.L., X.L. and D.M..

Conflict of Interests

The authors declare no competing interests.

Data Availability Statement

All data and materials used in the analysis are available to any researcher for purposes of reproducing or extending the analysis.

References

1. Xu F, Li W, Yang X, Na L, Chen L, Liu G: **The Roles of Epigenetics Regulation in Bone**

Metabolism and Osteoporosis. *Front Cell Dev Biol* 2020, **8:**619301.

2. Mikosch P: **Alcohol and bone.** *Wien Med Wochenschr* 2014, **164:**15-24.
3. Ulhoi MP, Meldgaard K, Steiniche T, Odgaard A, Vesterby A: **Chronic Alcohol Abuse Leads to Low Bone Mass with No General Loss of Bone Structure or Bone Mechanical Strength<sup/>.** *J Forensic Sci* 2017, **62:**131-136.
4. Berg KM, Kunins HV, Jackson JL, Nahvi S, Chaudhry A, Harris KA, Jr., Malik R, Arnsten JH: **Association between alcohol consumption and both osteoporotic fracture and bone density.** *Am J Med* 2008, **121:**406-418.
5. Grosso A, Burger MG, Lunger A, Schaefer DJ, Banfi A, Di Maggio N: **It Takes Two to Tango: Coupling of Angiogenesis and Osteogenesis for Bone Regeneration.** *Front Bioeng Biotechnol* 2017, **5:**68.
6. Kusumbe AP, Ramasamy SK, Adams RH: **Coupling of angiogenesis and osteogenesis by a specific vessel subtype in bone.** *Nature* 2014, **507:**323-328.
7. Zhang J, Pan J, Jing W: **Motivating role of type H vessels in bone regeneration.** *Cell Prolif* 2020, **53:**e12874.
8. Watson EC, Adams RH: **Biology of Bone: The Vasculature of the Skeletal System.** *Cold Spring Harb Perspect Med* 2018, **8**.
9. Wang G, Nie JH, Bao Y, Yang X: **Sulforaphane Rescues Ethanol-Suppressed Angiogenesis through Oxidative and Endoplasmic Reticulum Stress in Chick Embryos.** *J Agric Food Chem* 2018, **66:**9522-9533.
10. Zhang Y, Yuan H, Sun Y, Wang Y, Wang A: **The effects of ethanol on angiogenesis after myocardial infarction, and preservation of angiogenesis with rosuvastatin after heavy drinking.** *Alcohol* 2016, **54:**27-32.
11. Wang G, Zhong S, Zhang SY, Ma ZL, Chen JL, Lu WH, Cheng X, Chuai M, Lee KK, Lu DX, Yang X: **Angiogenesis is repressed by ethanol exposure during chick embryonic development.** *J Appl Toxicol* 2016, **36:**692-701.
12. Chen H, Chen H, Liang J, Gu X, Zhou J, Xie C, Lv X, Wang R, Li Q, Mao Z, et al: **TGF-beta1/IL-11/MEK/ERK signaling mediates senescence-associated pulmonary fibrosis in a stress-induced premature senescence model of Bmi-1 deficiency.** *Exp Mol Med* 2020, **52:**130-151.
13. Liu J, Cao L, Chen J, Song S, Lee IH, Quijano C, Liu H, Keyvanfar K, Chen H, Cao LY, et al: **Bmi1 regulates mitochondrial function and the DNA damage response pathway.** *Nature* 2009, **459:**387-392.
14. Jin J, Lv X, Chen L, Zhang W, Li J, Wang Q, Wang R, Lu X, Miao D: **Bmi-1 plays a critical role in protection from renal tubulointerstitial injury by maintaining redox balance.** *Aging Cell* 2014, **13:**797-809.
15. Zhang HW, Ding J, Jin JL, Guo J, Liu JN, Karaplis A, Goltzman D, Miao D: **Defects in mesenchymal stem cell self-renewal and cell fate determination lead to an osteopenic phenotype in Bmi-1 null mice.** *J Bone Miner Res* 2010, **25:**640-652.
16. Huber LC, Ulrich S, Leuenberger C, Gassmann M, Vogel J, von Blotzheim LG, Speich R, Kohler M, Brock M: **Featured Article: microRNA-125a in pulmonary hypertension: Regulator of a proliferative phenotype of endothelial cells.** *Exp Biol Med (Maywood)* 2015, **240:**1580-1589.
17. Yang CS, Mercer KE, Alund AW, Suva LJ, Badger TM, Ronis MJ: **Genistein supplementation**

increases bone turnover but does not prevent alcohol-induced bone loss in male mice. *Exp Biol Med (Maywood)* 2014, **239:**1380-1389.

18. Sun H, Qiao W, Cui M, Yang C, Wang R, Goltzman D, Jin J, Miao D: **The Polycomb Protein Bmi1 Plays a Crucial Role in the Prevention of 1,25(OH)2 D Deficiency-Induced Bone Loss.** *J Bone Miner Res* 2020, **35:**583-595.
19. Yu W, Zhong L, Yao L, Wei Y, Gui T, Li Z, Kim H, Holdreith N, Jiang X, Tong W, et al: **Bone marrow adipogenic lineage precursors promote osteoclastogenesis in bone remodeling and pathologic bone loss.** *J Clin Invest* 2021, **131**.
20. Bian Y, Du Y, Wang R, Chen N, Du X, Wang Y, Yuan H: **A comparative study of HAMSCs/HBMSCs transwell and mixed coculture systems.** *IUBMB Life* 2019, **71:**1048-1055.
21. Ma Q, Liang M, Wu Y, Luo F, Ma Z, Dong S, Xu J, Dou C: **Osteoclast-derived apoptotic bodies couple bone resorption and formation in bone remodeling.** *Bone Res* 2021, **9:**5.
22. Miao D, Bai X, Panda D, McKee M, Karaplis A, Goltzman D: **Osteomalacia in hyp mice is associated with abnormal phex expression and with altered bone matrix protein expression and deposition.** *Endocrinology* 2001, **142:**926-939.
23. Zhang ZL, Tong J, Lu RN, Scutt AM, Goltzman D, Miao DS: **Therapeutic potential of non-adherent BM-derived mesenchymal stem cells in tissue regeneration.** *Bone Marrow Transplant* 2009, **43:**69-81.
24. Zhou J, Chen A, Wang Z, Zhang J, Chen H, Zhang H, Wang R, Miao D, Jin J: **Bmi-1 determines the stemness of renal stem or progenitor cells.** *Biochem Biophys Res Commun* 2020, **529:**1165-1172.
25. Xie C, Jin J, Lv X, Tao J, Wang R, Miao D: **Anti-aging Effect of Transplanted Amniotic Membrane Mesenchymal Stem Cells in a Premature Aging Model of Bmi-1 Deficiency.** *Sci Rep* 2015, **5:**13975.
26. Schafer S, Viswanathan S, Widjaja AA, Lim WW, Moreno-Moral A, DeLaughter DM, Ng B, Patone G, Chow K, Khin E, et al: **IL-11 is a crucial determinant of cardiovascular fibrosis.** *Nature* 2017, **552:**110-115.
27. Zura R, Xiong Z, Einhorn T, Watson JT, Ostrum RF, Prayson MJ, Della Rocca GJ, Mehta S, McKinley T, Wang Z, Steen RG: **Epidemiology of Fracture Nonunion in 18 Human Bones.** *JAMA Surg* 2016, **151:**e162775.
28. Chakkalakal DA: **Alcohol-induced bone loss and deficient bone repair.** *Alcohol Clin Exp Res* 2005, **29:**2077-2090.
29. Ilich JZ, Brownbill RA, Tamborini L, Crncevic-Orlic Z: **To drink or not to drink: how are alcohol, caffeine and past smoking related to bone mineral density in elderly women?** *J Am Coll Nutr* 2002, **21:**536-544.
30. de Souza DM, Rodrigues VA, Silva AA, Gonsalves VS, Pereira KA, Nishioka RS, de Carvalho C: **Influence of different alcohol intake frequencies on alveolar bone loss in adult rats: A sem study.** *J Clin Exp Dent* 2018, **10:**e852-e857.
31. Gaddini GW, Turner RT, Grant KA, Iwaniec UT: **Alcohol: A Simple Nutrient with Complex Actions on Bone in the Adult Skeleton.** *Alcohol Clin Exp Res* 2016, **40:**657-671.
32. Fu R, Lv WC, Xu Y, Gong MY, Chen XJ, Jiang N, Xu Y, Yao QQ, Di L, Lu T, et al: **Endothelial ZEB1 promotes angiogenesis-dependent bone formation and reverses osteoporosis.** *Nat Commun* 2020, **11:**460.

33. Yin Y, Tang Q, Xie M, Hu L, Chen L: **Insights into the mechanism of vascular endothelial cells on bone biology.** *Biosci Rep* 2021, **41**.
34. Liu X, Zhang Y, Liu L, Zhu S: **Transcriptomic-based toxicological investigations of ethanol to human umbilical vein endothelial cells.** *J Appl Toxicol* 2021, **41:**736-744.
35. Chen Y, Yu H, Zhu D, Liu P, Yin J, Liu D, Zheng M, Gao J, Zhang C, Gao Y: **miR-136-3p targets PTEN to regulate vascularization and bone formation and ameliorates alcohol-induced osteopenia.** *FASEB J* 2020, **34:**5348-5362.
36. Andres V: **Control of vascular cell proliferation and migration by cyclin-dependent kinase signalling: new perspectives and therapeutic potential.** *Cardiovasc Res* 2004, **63:**11-21.
37. Gu X, Peng CY, Lin SY, Qin ZY, Liang JL, Chen HJ, Hou CX, Wang R, Du YQ, Jin JL, Yang ZJ: **P16(INK4a) played a critical role in exacerbating acute tubular necrosis in acute kidney injury.** *Am J Transl Res* 2019, **11:**3850-3861.
38. Chen G, Deng C, Li YP: **TGF-beta and BMP signaling in osteoblast differentiation and bone formation.** *Int J Biol Sci* 2012, **8:**272-288.
39. Kamiya N: **The role of BMPs in bone anabolism and their potential targets SOST and DKK1.** *Curr Mol Pharmacol* 2012, **5:**153-163.
40. Hendriks M, Ramasamy SK: **Blood Vessels and Vascular Niches in Bone Development and Physiological Remodeling.** *Front Cell Dev Biol* 2020, **8:**602278.
41. Canalis E, Economides AN, Gazzerro E: **Bone morphogenetic proteins, their antagonists, and the skeleton.** *Endocr Rev* 2003, **24:**218-235.
42. Ambrosi TH, Marecic O, McArdle A, Sinha R, Gulati GS, Tong XM, Wang YT, Steininger HM, Hoover MY, Koepke LS, et al: **Aged skeletal stem cells generate an inflammatory degenerative niche.** *Nature* 2021.
43. Garrison KR, Shemilt I, Donell S, Ryder JJ, Mugford M, Harvey I, Song F, Alt V: **Bone morphogenetic protein (BMP) for fracture healing in adults.** *Cochrane Database Syst Rev* 2010**:**CD006950.
44. Hak DJ: **Management of aseptic tibial nonunion.** *J Am Acad Orthop Surg* 2011, **19:**563-573.
45. Bratton A, Eisenberg J, Vuchkovska A, Roper P, Callaci JJ: **Effects of Episodic Alcohol Exposure on BMP2 Signaling During Tibia Fracture Healing.** *J Orthop Trauma* 2018, **32:**288-295.

Figure legends

Figure 1 The alcoholic diet retards the bone growth and leads to osteoporosis in mice

The experiments were carried out on the two-month-old mice fed with normal diet or alcoholic diet for two months. The tibias were isolated and analyzed with X-ray and micro-CT. Paraffin-embedded tibial sections from four-month-old normal- and alcohol-

diet mice were prepared. (A) Representative micrographs of X-ray for tibias. (B) Quantification of tibial length (cm). (C) Representative micrographs of Safranin O/fast green staining. (D) Quantification of femoral growth plate thickness (μm). (E) Representative micrographs of PCNA immunostaining (labeled with blue arrows) with tibial sections (F) Quantification of number of PCNA positive chondrocytes in the growth plate of tibial. (G) Representative three-dimensional reconstruction of micro-CT of tibias. (H) Representative micrographs of total collagen staining with tibial sections. (I) Quantitative histomorphometry analysis of bone mineral density (BMD) (mg/cm^3), bone volume relative to tissue volume (BV/TV) (%), trabecular separation (Tb.Sp) (μm), trabecular number (Tb.N) (μm^{-1}) and trabecular thickness (Tb.Th) (μm) from tibias. Six mice per group were used for experiments. Statistical analysis was performed with *t* test. Values are mean ± SEM from six determinations per group, *:$P<0.05$; **:$P < 0.01$ compared with normal-diet mice.

Figure 2 The alcoholic diet impairs bone formation of osteoblasts in mice

The experiments were carried out on the two-month-old mice fed with normal diet or alcoholic diet for two months. Paraffin-embedded or frozen tibial sections from four-month-old normal- or alcohol-diet mice were prepared and used for immunohistochemical or immunofluorescence staining respectively. (A) Representative micrographs of Runx2 immunostaining (labeled with white arrows) in tibial sections, with DAPI staining the nuclei. (B) Quantification of areas of Runx2 positive osteoblasts in tibias. (C) Representative micrographs of type-1-collahen

(collagen 1) immunostaining with tibial sections. (D) Quantification of areas of collagen 1 in tibias. (E) Western blots of tibial lysates for expression of Bmp2, Osterix, Runx2 and alkaline phosphatase (ALP); β-actin was used as the loading control. (F) Protein levels relative to β-actin protein levels were assessed by densitometric analysis. Six mice per group were used for experiments. Statistical analysis was performed with *t* test. Values are mean ± SEM from six determinations per group, *: $P < 0.05$; **: $P<0.01$; ***: $P < 0.001$ compared with normal-diet mice.

Figure 3 The alcoholic diet impairs CD31^{hi}EMCN^{hi} type-H-vessel formation through inhibiting proliferation and promoting aging of endothelial cells

The experiments were carried out on the two-month-old mice fed with normal diet or alcoholic diet for two months. Frozen tibial sections from four-month-old normal- and alcohol-diet mice were prepared and used for immunofluorescence staining. (A) Representative micrographs showing immunofluorescence for CD31 (green), EMCN (red) and Osterix (white), with DAPI staining the nuclei. (B) Number of CD31^{hi}EMCN^{hi} endothelial cells (Type-H ECs) (labeled with white arrows). Six mice per group were used for experiments. Statistical analysis was performed with *t* test. Values are mean ± SEM from six determinations per group, *: $P < 0.05$ compared with normal-diet mice. HUVECs were treated with 0%, 0.5%, 3% or 5% alcohol for 12 hours. (C) Representative micrographs for Matrigel tube formation assay. (D) Cumulative tube length of HUVECs treated without or with different-concentrated alcohol (0.5%, 3% and 5%). (E) HUVECs viability was respectively assessed at 0, 24, or 48 h after

treatment with different-concentrated alcohol (0.15%, 0.5%, 3% and 5%). (F) Representative micrographs of immunofluorescence for p16, with DAPI staining the nuclei. (G) P16 positive cells (%). (H) Western blots of cell lysates for Bmi-1, CDK6, Cyclin D and E2F1; β-actin was used as the loading control. (I) Protein levels relative to β-actin protein levels were assessed by densitometric analysis. Cell experiments were performed with three biological repetitions per group. Statistical analysis was performed with One-way ANOVA test. Values are mean ± SEM from three determinations per group, $^{*}P < 0.05$; $^{**}P < 0.01$; $^{***}P < 0.001$ compared with vehicle group; $^{\#\#}P < 0.01$; $^{\#\#\#}P < 0.001$ compared with 0.5%-alcohol-treated group; $^{\&}P < 0.05$; $^{\&\&}P < 0.01$; $^{\&\&\&}P < 0.001$ compared with 3%-alcohol-treated group.

Figure 4 Alcohol inhibits the differentiation of BM-MSCs into osteoblasts through reducing the BMP2 secretion of endothelial cells in type-H vessels

HUVECs were respectively treated with 0%, 0.5%, 3% or 5% alcohol for 12 hours. The conditioned medium of the above HUVECs cells was collected to culture hBM-MSCs and induce them to differentiate into osteoblasts *in vitro*. (A) Representative micrographs of alkaline phosphatase (ALP) staining. (B) ALP positive areas (%). (C) Representative micrographs of Alizarin red S staining. (D) Quantitative analysis of calcium deposits in hBM-MSCs. Cell experiments were performed with three biological repetitions per group. Statistical analysis was performed with One-way ANOVA test. Values are mean ± SEM from three determinations per group, $^{***}P < 0.001$ compared with vehicle group; $^{\#\#\#}P < 0.001$ compared with 0.5%-alcohol-treated group;

$^{\&\&}$P<0.01 compared with 3%-alcohol-treated group. (E-G) Representative micrographs of immunofluorescence for CD31 and BMP2, Bmi-1 or p16 (labeled with white arrows) in frozen tibial sections from normal- and alcohol-diet mice, with DAPI staining the nuclei. (H) Quantitative analysis of cells adjacent to type-H vessels. Six mice per group were used for experiments. Statistical analysis was performed with *t* test. Values are mean ± SEM from six determinations per group, **P<0.01; ***P< 0.001 compared with normal-diet mice. HUVECs were treated with 0%, 0.5%, 3% or 5% alcohol for 12 hours. (I) Western blots of cell lysates for Bmp2; β-actin was used as the loading control. (I) Protein levels relative to β-actin protein levels were assessed by densitometric analysis. Cell experiments were performed with three biological repetitions per group. Statistical analysis was performed with One-way ANOVA test. Values are mean ± SEM from three determinations per group, ***P< 0.001 compared with vehicle group; $^{\#\#\#}$P < 0.001 compared with 0.5%-alcohol-treated group; $^{\&\&}$P<0.01 compared with 3%-alcohol-treated group.

Figures

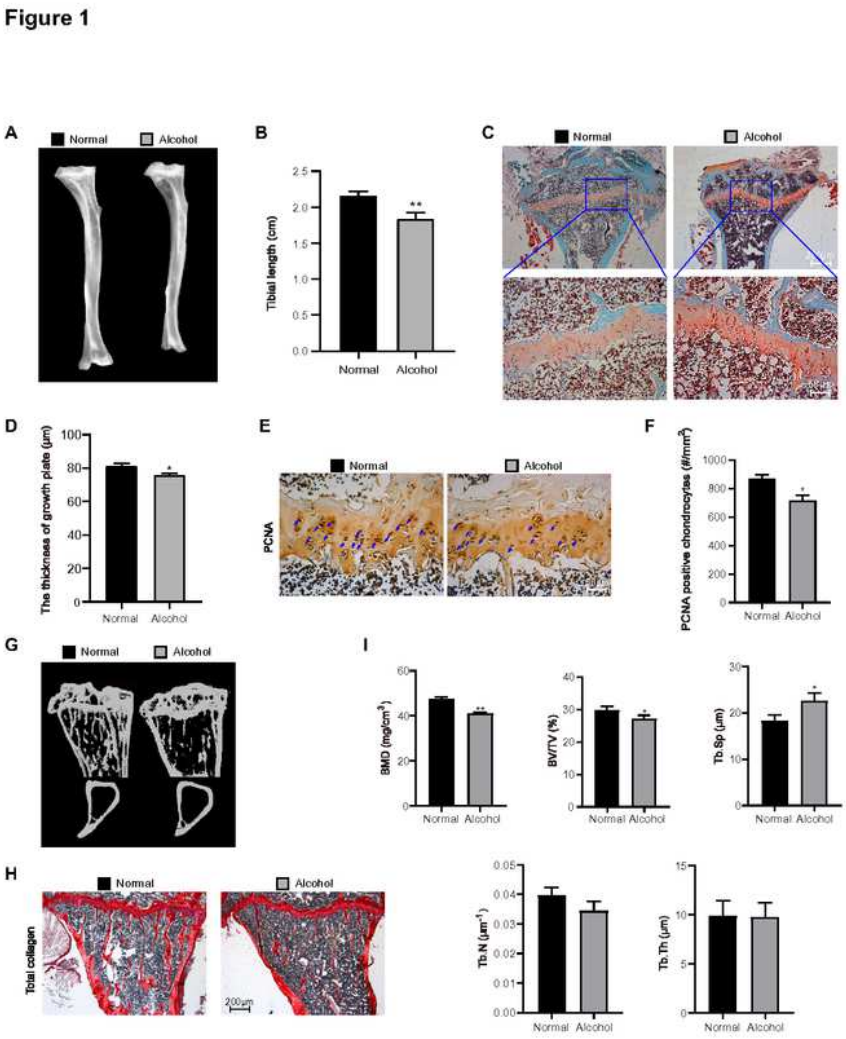

Figure 1

The alcoholic diet retards the bone growth and leads to osteoporosis in mice The experiments were carried out on the two-month-old mice fed with normal diet or alcoholic diet for two months. The tibias were isolated and analyzed with X-ray and micro-CT. Paraffin-embedded tibial sections from four-month-

old normal- and alcohol-diet mice were prepared. (A) Representative micrographs of X-ray for tibias. (B) Quantification of tibial length (cm). (C) Representative micrographs of Safranin O/fast green staining. (D) Quantification of femoral growth plate thickness (μm). (E) Representative micrographs of PCNA immunostaining (labeled with blue arrows) with tibial sections (F) Quantification of number of PCNA positive chondrocytes in the growth plate of tibial. (G) Representative three-dimensional econstruction of micro-CT of tibias. (H) Representative micrographs of total collagen staining with tibial sections. (I) Quantitative histomorphometry analysis of bone mineral density (BMD) (mg/cm3), bone volume relative to tissue volume (BV/TV) (%), trabecular separation (Tb.Sp) (μm), trabecular number (Tb.N) (μm-1) and trabecular thickness (Tb.Th) (μm) from tibias. Six mice per group were used for experiments. Statistical analysis was performed with t test. Values are mean ± SEM from six determinations per group, *:$P<0.05$; **:$P < 0.01$ compared with normal-diet mice.

Figure 2

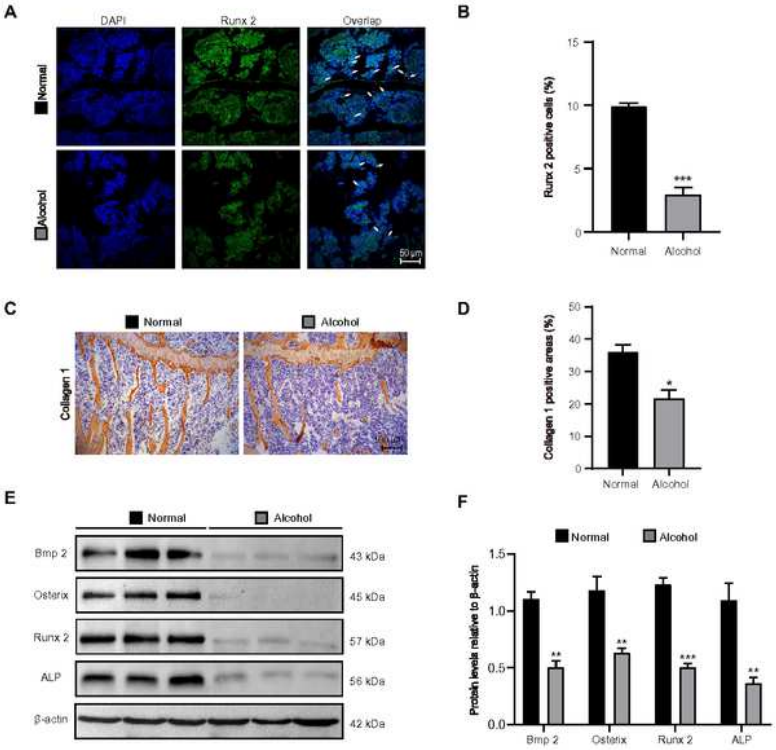

Figure 2

The alcoholic diet impairs bone formation of osteoblasts in mice The experiments were carried out on the two-month-old mice fed with normal diet or alcoholic diet for two months. Paraffin-embedded or frozen tibial sections from four-month-old normal- or alcohol-diet mice were prepared and used for immunohistochemical or immunofluorescence staining respectively. (A) Representative micrographs of Runx2 immunostaining (labeled with white arrows) in tibial sections, with DAPI staining the nuclei. (B)

Quantification of areas of Runx2 positive osteoblasts in tibias. (C) Representative micrographs of type-1-collahen (collagen 1) immunostaining with tibial sections. (D) Quantification of areas of collagen 1 in tibias. (E) Western blots of tibial lysates for expression of Bmp2, Osterix, Runx2 and alkaline phosphatase (ALP); β-actin was used as the loading control. (F) Protein levels relative to β-actin protein levels were assessed by densitometric analysis. Six mice per group were used for experiments. Statistical analysis was performed with t test. Values are mean ± SEM from six determinations per group, *: P < 0.05; **: P<0.01; ***: P < 0.001 compared with normal-diet mice.

Figure 3

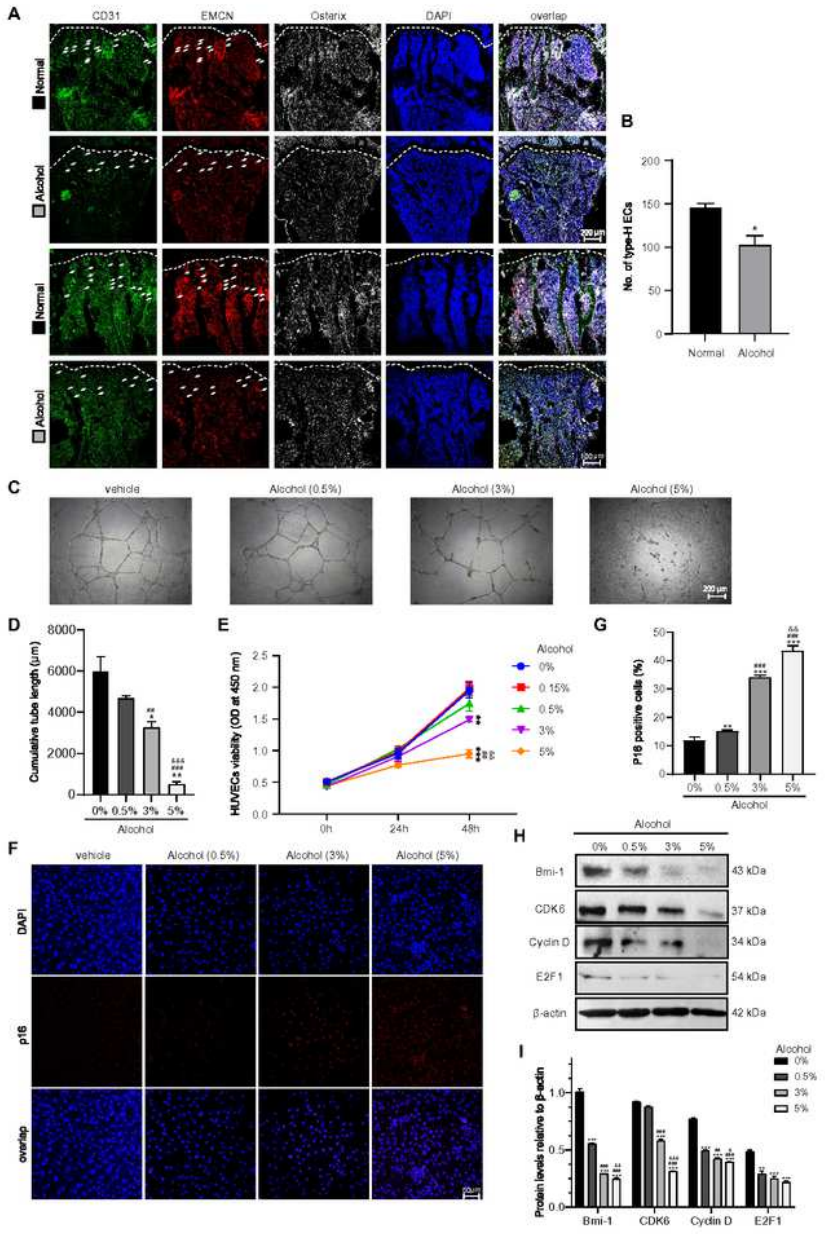

Figure 3

The alcoholic diet impairs CD31hiEMCNhi type-H-vessel formation through inhibiting proliferation and promoting aging of endothelial cells The experiments were carried out on the two-month-old mice fed with normal diet or alcoholic diet for two months. Frozen tibial sections from four-month-old normal- and alcohol-diet mice were prepared and used for immunofluorescence staining. (A) Representative micrographs showing immunofluorescence for CD31 (green), EMCN (red) and Osterix (white), with DAPI staining the nuclei. (B) Number of CD31hiEMCNhi endothelial cells (Type-H ECs) (labeled with white arrows). Six mice per group were used for experiments. Statistical analysis was performed with t test. Values are mean ± SEM from six determinations per group, *: $P < 0.05$ compared with normal-diet mice. HUVECs were treated with 0%, 0.5%, 3% or 5% alcohol for 12 hours. (C) Representative micrographs for Matrigel tube formation assay. (D) Cumulative tube length of HUVECs treated without or with different-concentrated alcohol (0.5%, 3% and 5%). (E) HUVECs viability was respectively assessed at 0, 24, or 48 h after treatment with different-concentrated alcohol (0.15%, 0.5%, 3% and 5%). (F) Representative micrographs of immunofluorescence for p16, with DAPI staining the nuclei. (G) P16 positive cells (%). (H) Western blots of cell lysates for Bmi-1, CDK6, Cyclin D and E2F1; β-actin was used as the loading control. (I) Protein levels relative to β-actin protein levels were assessed by densitometric analysis. Cell experiments were performed with three biological repetitions per group. Statistical analysis was performed with One-way ANOVA test. Values are mean ± SEM from three determinations per group, *$P < 0.05$; **$P < 0.01$; ***$P < 0.001$ compared with vehicle group; ##$P < 0.01$; ###$P < 0.001$ compared with 0.5%-alcohol-treated group; &$P < 0.05$; &&$P < 0.01$; &&&$P < 0.001$ compared with 3%-alcohol-treated group.

Figure 4

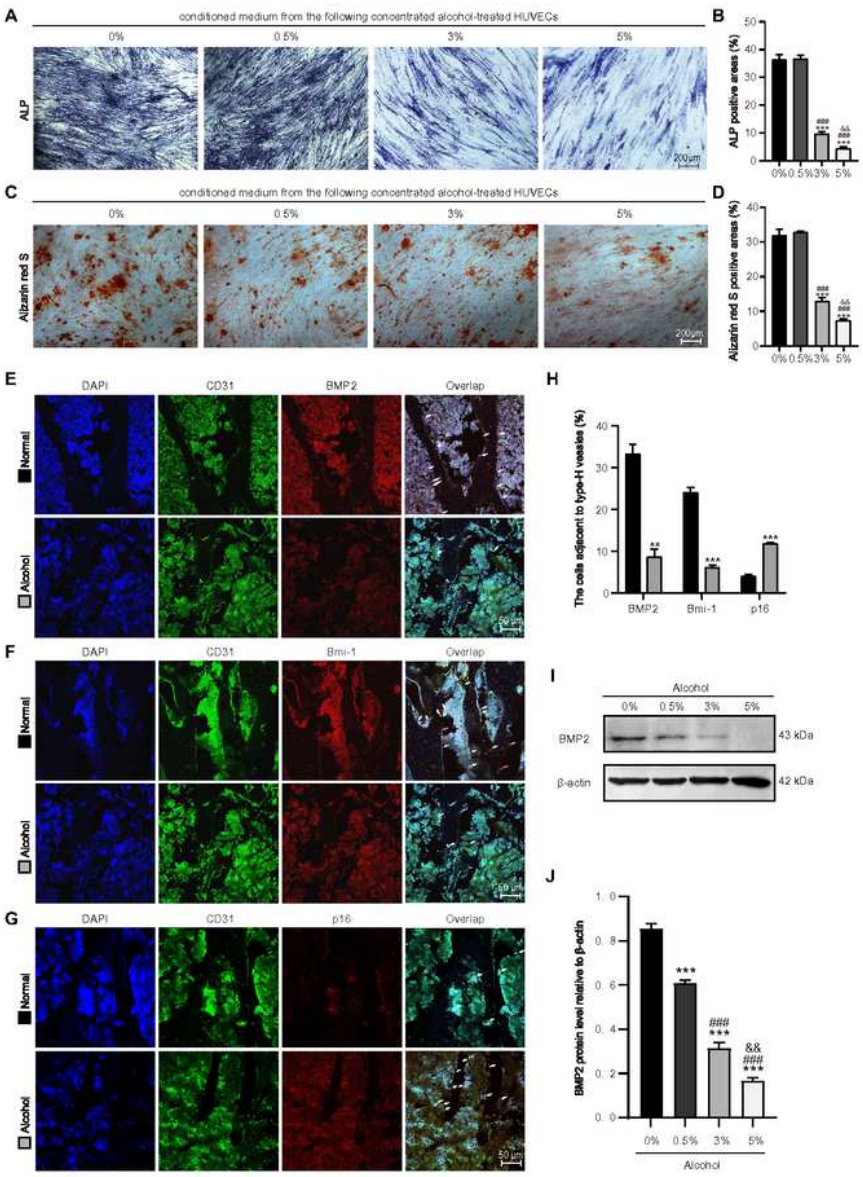

Figure 4

Alcohol inhibits the differentiation of BM-MSCs into osteoblasts through reducing the BMP2 secretion of endothelial cells in type-H vessels HUVECs were respectively treated with 0%, 0.5%, 3% or 5% alcohol for 12 hours. The conditioned medium of the above HUVECs cells was collected to culture hBM-MSCs and induce them to differentiate into osteoblasts in vitro. (A) Representative micrographs of alkaline phosphatase (ALP) staining. (B) ALP positive areas (%). (C) Representative micrographs of Alizarin red S

staining. (D) Quantitative analysis of calcium deposits in hBM-MSCs. Cell experiments were performed with three biological repetitions per group. Statistical analysis was performed with One-way ANOVA test. Values are mean ± SEM from three determinations per group, ***P <0.001 compared with vehicle group; ###P <0.001 compared with 0.5%-alcohol-treated group; &&P<0.01 compared with 3%-alcohol-treated group. (E-G) Representative micrographs of immunofluorescence for CD31 and BMP2, Bmi-1 or p16 (labeled with white arrows) in frozen tibial sections from normal- and alcohol-diet mice, with DAPI staining the nuclei. (H) Quantitative analysis of cells adjacent to type-H vessels. Six mice per group were used for experiments. Statistical analysis was performed with t test. Values are mean ± SEM from six determinations per group, **P<0.01; ***P< 0.001 compared with normal-diet mice. HUVECs were treated with 0%, 0.5%, 3% or 5% alcohol for 12 hours. (I) Western blots of cell lysates for Bmp2; β-actin was used as the loading control. (I) Protein levels relative to β-actin protein levels were assessed by densitometric analysis. Cell experiments were performed with three biological repetitions per group. Statistical analysis was performed with One-way ANOVA test. Values are mean ± SEM from three determinations per group, ***P< 0.001 compared with vehicle group; ###P < 0.001 compared with 0.5%-alcohol-treated group; &&P<0.01 compared with 3%-alcohol-treated group.

Supplementary Files

This is a list of supplementary files associated with this preprint. Click to download.

- GraphicalAbstract.pdf